The II–I crystal transformation of poly(vinylidene fluoride) under tensile and compressional stresses

K. Matsushige, K. Nagata, S. Imada, and T. Takemura
Department of Applied Science, Faculty of Engineering, Kyushu University, Fukuoka 812, *Japan*
(*Received* 23 *October* 1979)

The mechanism for a crystal transformation in poly(vinylidene fluoride) by a tensile deformation at atmospheric pressure was investigated in the temperature range 25–150 °C. Simultaneous X-ray and stress–strain relationship measurements during the drawing process revealed that the crystal transformation from Form II to Form I occurred at the temperatures below 130°C where the sample deformed by cold-drawing, and always initiated at the deformation stage where necking was completed at the centre of the tensile sample. Above 140°C, on the other hand, the sample deformed uniformly without necking and did not perform the crystal transformation. Thus, it was suggested that a heterogeneous stress distribution in the sample played a critically important role in the crystal transformation phenomenon. A uniaxial compressional deformation also caused the crystal transformation from Form II to Form I in this sample. The crystal conversion ratio varied with the conditions of compressional pressure and temperature, and the molecular orientation in resultant samples depended on the shapes of the anvils employed in the compression experiment. By applying a high d.c. voltage during the compressional deformation, a highly uniaxially oriented Form I film with prominent piezoelectric properties was obtained.

INTRODUCTION

Poly(vinylidene fluoride), PVDF, is a polymeric material with very interesting scientific and technological properties. This polymer is known to crystallize into three different crystal forms, denoted I (β), II (α), and III (γ), depending upon crystallization conditions, and to perform mutual crystal transformations between these crystal forms[1–10]. Among these crystal forms, Form I crystal contains a large spontaneous polarization in its unit cell[5–8] and when oriented and then poled under a high d.c. electric field exhibits the highest piezoelectric properties in synthetic polymers[11]. In recent years, therefore, the studies of the methods of preparing oriented Form I crystal with a high degree of crystal perfection[12,13] as well as application of PVDF piezoelectric films to engineering devices have attracted many researchers. The oriented Form I crystal is usually obtained by the drawing of Form II crystal at atmospheric pressure. On this II–I crystal transformation by drawing, Lando *et al.*[4] reported that a drawing temperature determines relative contents of Form I and Form II crystal in the drawn sample. However, the detailed correlation between the deformation mechanism and the II–I crystal transformation phenomenon is still unknown.

In this study, the changes in X-ray diffraction patterns occurring during the drawing process were followed simultaneously with a tensile stress–strain measurement at various drawing temperatures, and the deformation mechanism which plays an essential role for the crystal transformation was investigated. Furthermore, it was found that uniaxial compression also causes the II–I crystal transformation. By this method, an orientation and a poling procedure could be achieved simultaneously, resulting in a high piezoelectric Form I crystal film.

EXPERIMENTAL

The X-ray measuring system for observing a crystal transformation process of PVDF taking place during a drawing procedure is shown schematically in *Figure* 1. In order to study this process directly, a strong rotating anode X-ray generator (60 kV, 200 mA) and a PSPC (position sensitive proportional counter, manufactured by Rigaku Denki Co.) probe were used as an X-ray generator

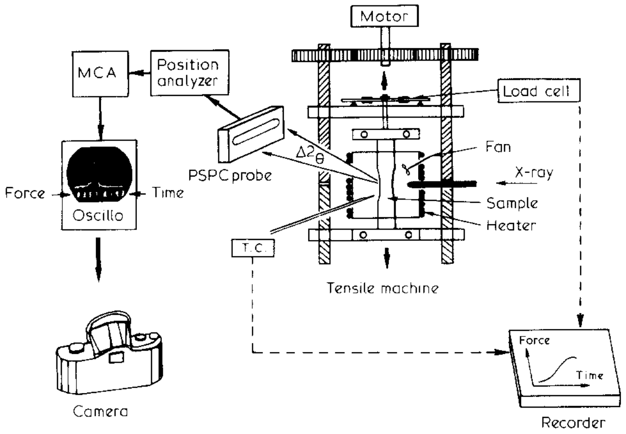

Figure 1 A schematic diagram of the X-ray system for observing a crystal transformation during drawing process. A stress–strain curve is simultaneously measured

0032–3861/80/1391–07$02.00

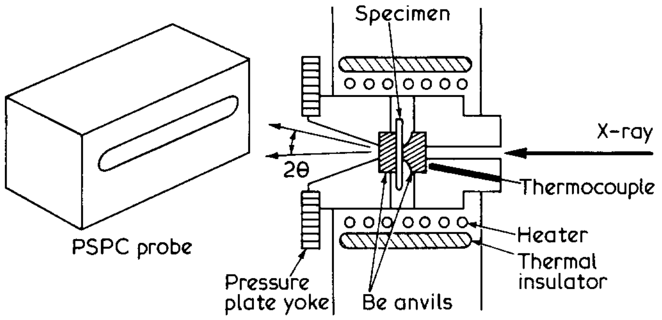

Figure 2 A schematic view of the X-ray system for observing a crystal transformation during an uniaxial compression process

and a detector, respectively. The PSPC system could analyse simultaneously the positions and intensities of X-ray beam reflected from a sample and collected data were displayed on an oscillograph. A counting time of the reflection pattern induced by CuKα radiation from the generator (37.5 kV, 100 mA) was $\sim$4 s, and the total time for one X-ray experiment including the time for taking a photograph with a camera was $\sim$6 s in this experiment. A tensile machine was specially designed. A driving force was generated by a synchronous motor, by which the strain rate was kept at a constant value of 5% min^{-1}. The sample holders were designed to move in opposite directions so that a X-ray beam spot did not transfer from the centre of samples even during a drawing process. The load applied to the sample was detected with a load cell made of strain gauges and a phosphor bronze plate, which was connected to an upper sample holder. The sample was set in an oven. The temperature in the oven was controlled with a heater and circulating fan, and monitored with an alumel–chromel thermocouple. The dimensional changes in the tensile sample taking place during the drawing process were also measured optically in a separate draw experiment under the same conditions and the data were utilized to calculate true stress–strain relationships from the observed nominal stress–strain curves.

Figure 2 shows a schematic view of the X-ray measuring system for the crystal transformation process during uniaxial compression procedure. The NBS type diamond anvil apparatus (manufactured at High Pressure Diamond Optics Inc.) was modified for this experiment. The pistons and beryllium metal anvils (one anvil is a cylinder of 6 mm^{ϕ} and the other has a surface of 3 mm^{ϕ}) were designed for this purpose. The temperature of the compression apparatus could be controlled with a heater wound around the inner cylinder and monitored with a thermocouple inserted in the piston. Compression moulded samples with large dimensions were necessary for the i.r. and piezoelectric measurements and the compression apparatus shown in *Figure* 3 was employed. The anvils were made of hardened alloy steel and their surfaces were either circular (13 mm^{ϕ}) or rectangular (6 mm x 30 mm). A compressional force was generated with a 50 ton press and applied to the anvils. In this apparatus, both the anvils were electrically insulated from each other, enabling the application of a high d.c. voltage to be made to the sample even during a compression cycle.

In this study, KF-polymer films (50 μm and 500 μm in thickness) with number-average molecular weight of 54 000, supplied by Kureha Chemical Industry Co. were used as original Form II crystal samples. These films were confirmed by X-ray and i.r. (a JASCO model i.r.–G spectrometer) measurements to be Form II crystal sample with almost no Form I crystal content.

RESULTS AND DISCUSSION

Crystal transformation during drawing at atmospheric pressure

Drawing experiments were performed in the temperature range 75–150°C at atmospheric pressure. *Figure* 4 shows a nominal stress–strain curve observed at 75°C and the X-ray diffraction patterns taken at various deformation stages. The observed stress–strain relationship revealed that the sample underwent yielding, necking, and strain hardening as its strain increased. Also, the observed changes in the X-ray diffraction patterns revealed the detailed crystallographic nature of the crystal transformation from Form II to Form I, as described below. An appearance of Form I [200] and [110] combined reflection was detected at the stage 3, as indicated by an arrow in the third picture. At this deformation stage the necking was initiated at the centre of a tensile sample and started to propagate to both sample ends. With further increasing strain, an apparent peak angle of the main reflection exhibited a gradual shifting from 20.1° (the diffraction angle of Form II [110] reflection) to 20.8° (the one expected for Form I [200] and [110] combined reflection), and simultaneously a narrowing of its half height width. In contrast to the progressive development and completion of Form I crystal during the drawing process, the other [020], [100], and [021] reflections from Form II crystal diminished in their intensities with increasing strain. A further numerical analysis on the changes in the X-ray diffraction patterns observed at 75°C during the drawing process is shown in *Figure* 5, where an abscissa represents the peak angle of the main reflection and I_0 is an integrated intensity of the main reflection calculated from its peak area and is used as a normalization factor. The samples labelled 1–6 and *A* correspond to the samples deformed up to the stages 1–6 shown in *Figure* 4, and the sample prepared by an annealing at 4000 kg cm^{-2}, which was regarded as the most complete Form I crystal[13], respectively. With a shifting of the main re-

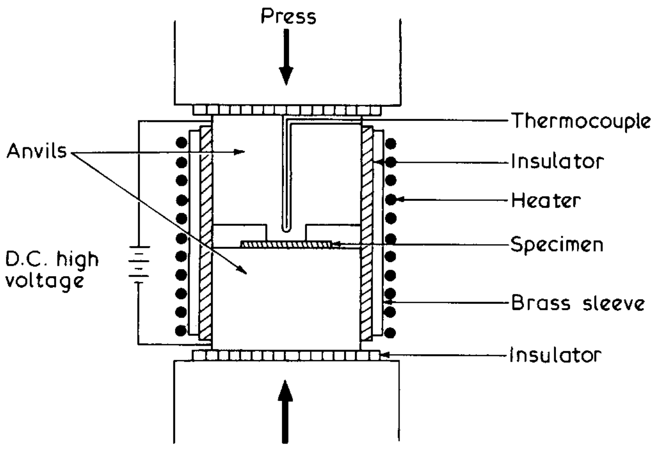

Figure 3 A conventional compression apparatus. A high d.c. voltage can be applied to the sample simultaneously with a compressional procedure since both an upper and a lower anvil are electrically insulated from others

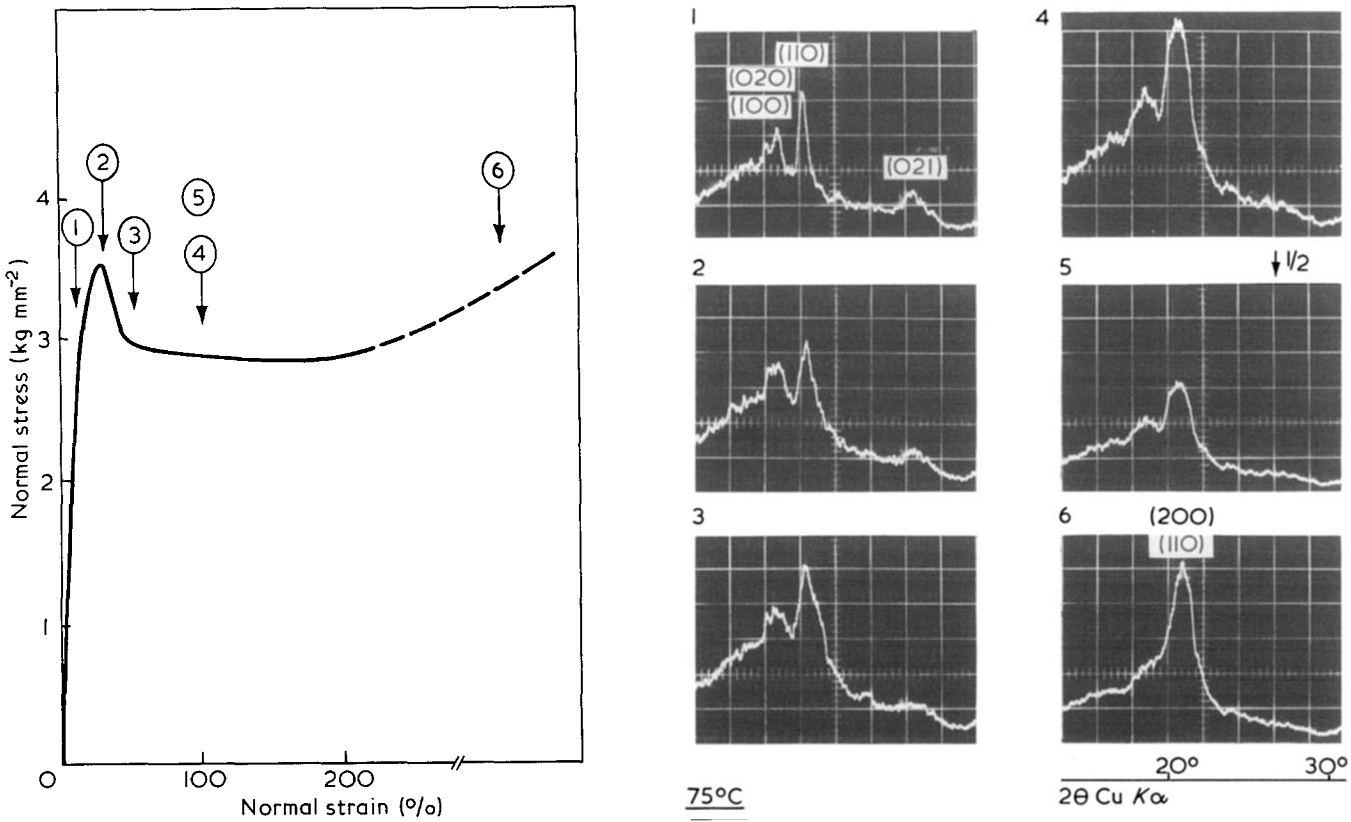

Figure 4 A normal stress–strain curve and X-ray diffraction patterns observed during a drawing experiment at 75°C. The X-ray diffraction pictures 1–6 were taken at the deformation stages indicated by numbers 1–6 on the normal stress–strain curve, respectively. A vertical scale in the X-ray diffraction patterns 5 and 6 is reduced to a half

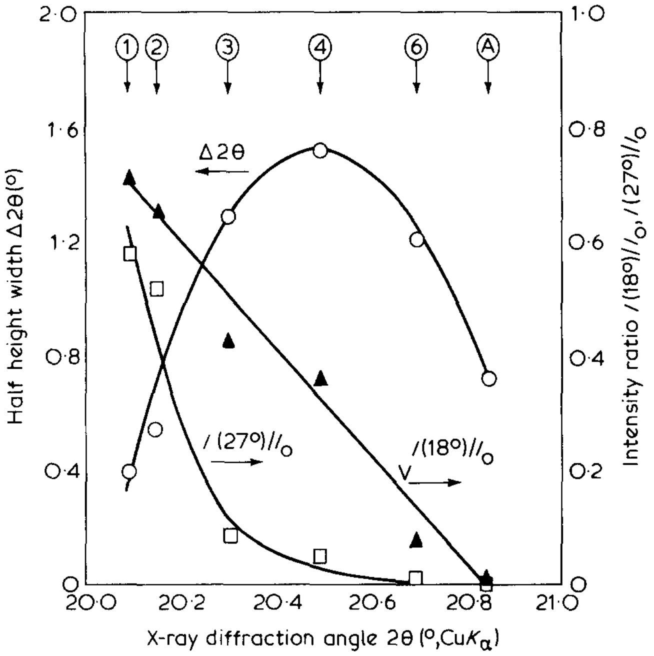

Figure 5 A numerical analysis of the X-ray diffraction patterns shown in *Figure 4*

flection toward 20.8°, the normalized intensity of Form II [021] reflection located around 27°, $I(27^\circ)/I_0$, exhibited a drastic decrease at an initial stage, while the combined intensity of Form II [100] and [020] reflections around 18°, $I(18^\circ)/I_0$, showed a linear decrease. However, a half-height width of the main reflection, $\Delta 2\theta$, exhibited a maximum value at a middle deformation stage, probably due to a coexistence of Form II [110] reflection and Form I [200] and [110] combined reflection. These facts suggest that *c*-axis molecular orientation proceeds to a high level at the initial drawing process and the crystal transformation from Form II to Form I proceeds in a rather continuous fashion, with the gradual reduction in the remaining Form II crystal content and a concomitant increase in the Form I crystal content with increasing strain.

Figure 6 shows the result observed at 150°C. In contrast to the case at 75°C, a nominal stress–strain curve did not exhibit any drop in stress above the yield point, suggesting that necking did not take place at this high temperature. Except for the [021] reflection, all the reflections from Form II crystal in the X-ray diffraction patterns were observed even at the highest strain level, while any reflection from Form I crystal could not be detected. This suggests that drawing at 150°C does not cause the crystal transformation, although *c*-axis orientation of Form II crystal proceeds to a high level as judged from a complete disappearance of Form II [021] reflection.

Similar drawing experiments were performed at different temperatures between 75°C and 150°C and the results are summarized in *Figures* 7 and 8. *Figure* 7 shows the nominal stress–strain curves observed at various temperatures. In the *Figure*, the information on an initiation point of the crystal transformation detected from X-ray diffraction experiments is also inserted. The crystal transformation from Form II to Form I was observed in the low temperature region below 130°C but not in the high temperature region above 140°C. It was also revealed that the degree of crystal conversion from Form II to Form I depended on the drawing temperature

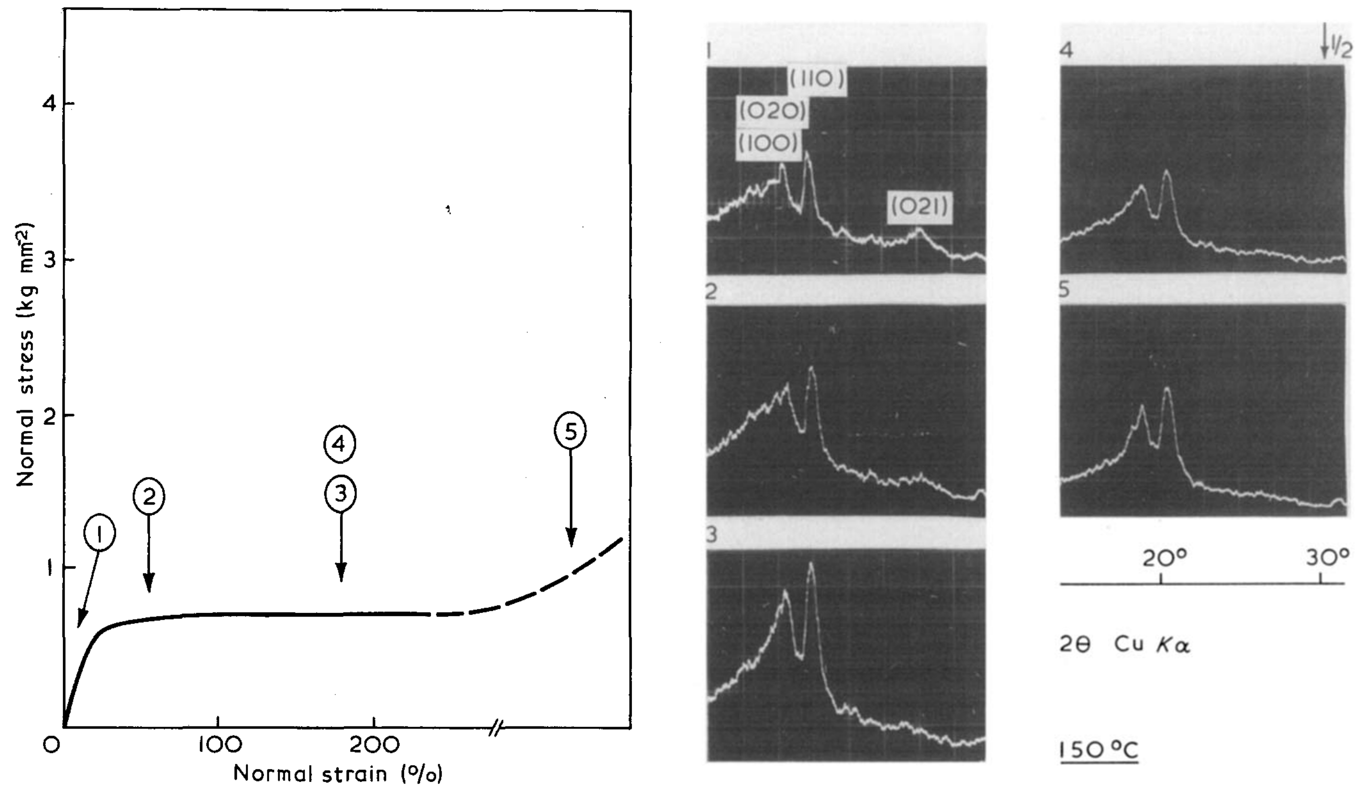

Figure 6 A normal stress–strain curve and X-ray diffraction patterns observed during a drawing experiment at 150°C

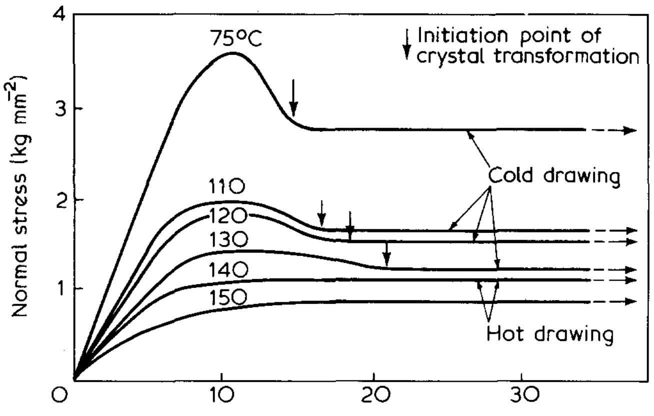

Figure 7 The normal stress–strain curves observed at different temperatures between 75 and 150°C. Arrows indicate the deformation stage where an initiation of the crystal transformation from Form II to Form I was detected by the X-ray experiments

and decreased with increasing drawing temperature. As indicated by arrows in the *Figure*, it is characteristic that the crystal transformation always initiated at the deformation stage where the necking was initiated at the centre of the tensile samples. Also, at the drawing temperature where the tensile deformation proceeded relatively uniformly such that a necking point could not be defined on the nominal stress–strain curves, the crystal transformation was not observed at all, even at a very high strain level. *Figure* 8 shows true stress–strain curves at different temperatures. In this *Figure*, however, no special feature can be identified to explain the effect of the drawing temperature on the crystal transformation phenomenon. Both the true stress and strain levels where the initiation of the crystal transformation was detected by the X-ray measurement varied with the drawing temperature, and no critical value existed in terms of true stress and strain.

As discussed above, a criterion determining whether the crystal transformation occurs or not seems to exist especially in the observed nominal stress–strain curves. That is, when the sample performs so-called 'cold drawing', crystal transformation takes place, whereas when the sample exhibits 'hot-drawing', it does not. Therefore, it has been observed that the drawing mechanism bears close correlation to the crystal transformation phenomenon and that the heterogeneous deformation process which recurs in cold drawing plays a critically important role in the crystal transformation phenomenon.

Crystal transformation upon uniaxial compression

The direct observations of structural changes occuring during an uniaxial compression process were performed at room temperature using a Be anvil compression apparatus. *Figure* 9 shows X-ray diffraction patterns under different compressional stress conditions. At atmospheric pressure X-ray reflections from Form II crystal as a starting sample was clearly detected. When the compressional stress was increased step by step and the X-ray diffraction pattern was examined at each occasion, a detectable decrease in intensities of Form II [100] and [110] reflections was observed at 3000 kg cm^{-2}. With further increase in the applied compressional stress, these reflections almost disappeared and other Form II [020] and [021] reflections became broad and less intense. On the other hand, a new reflection at $2\theta = \sim 21°$, which corresponds to Form I [200] and [110] combined reflection, could be clearly observed when the sample was annealed for 5 min at the condition of 155°C at atmos-

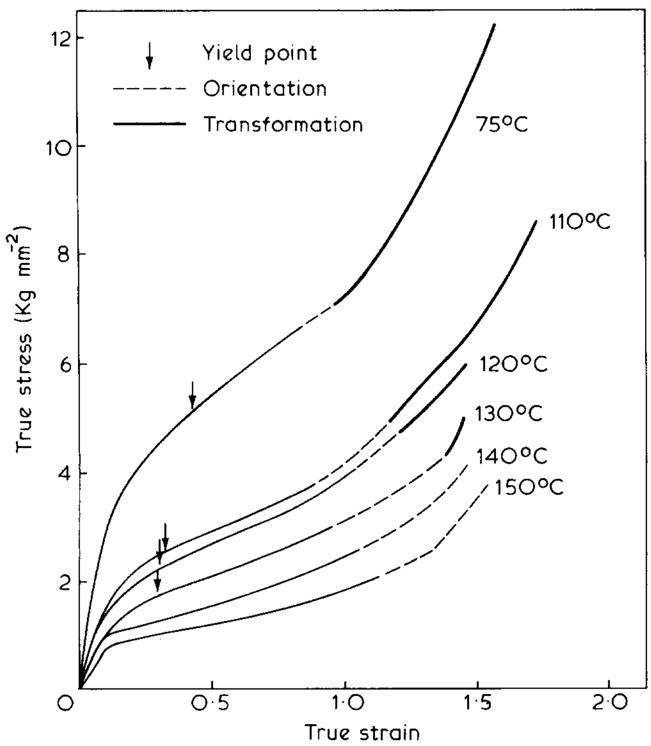

Figure 8 The true stress–strain curves for the samples drawn at different temperatures between 75 and 150°C. Arrows indicate the yield point defined as a maximum point on the normal stress–strain curves shown in *Figure 7*. The regions indicated by dotted and bold lines represent the deformation stages where *c*-axis molecular orientation and the crystal transformation, respectively, progressed, judging from the analysis of the observed X-ray diffraction patterns

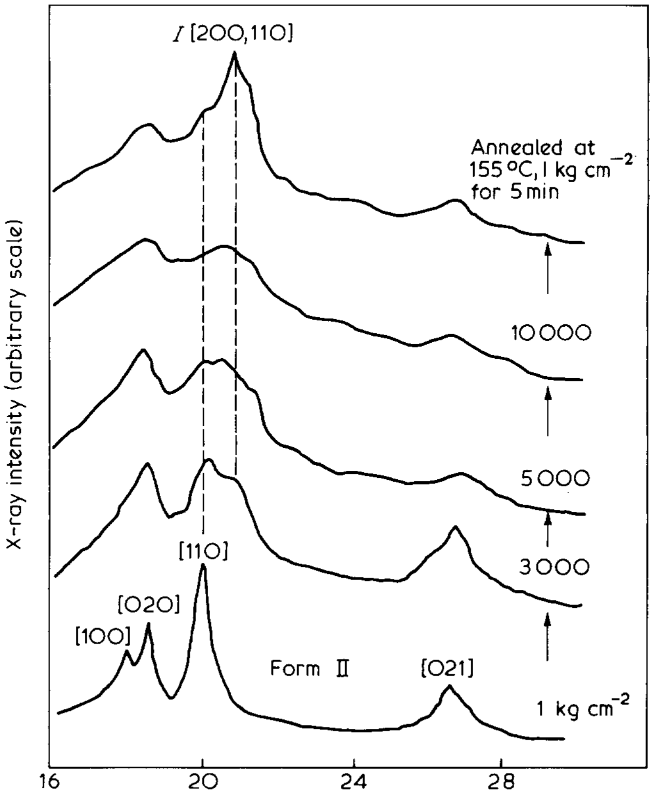

Figure 9 The X-ray diffraction patterns observed at various compressional stress conditions

pheric pressure. The X-ray diffraction patterns observed at high compressional stresses (5000 and 10 000 kg cm^{-2}) were diffuse due to the situation where the sample compressed with the Be anvils (whose shapes were circular), was deformed in radial directions as demonstrated and discussed later.

A reduction in sample thickness by the compression procedure was examined at the two temperatures, 25 and 125°C, in order to study whether or not the observed changes in X-ray diffraction patterns under compressional stresses are due to the crystal structure change induced by a plastic deformation (*Figure* 10). The measurement of thickness under compressional stresses was difficult and inaccurate, therefore, film samples with an original thickness of t_0 (500 μm) were compressed up to different stress levels, then the thickness of resultant samples, t, was measured at atmospheric pressure. In these experiments plastic deformation caused by the compression procedure could be detected only. When the sample was compressed at 25°C, the thickness reduction began at the stress level above 1000 kg cm^{-2} and its reduction rate became very slow above 3000 kg cm^{-2}. At a high compression temperature of 125°C, however, a drastic reduction in thickness occured at a much lower stress level just above 250 kg cm^{-2} and the resultant thickness of the sample compressed at 5000 kg cm^{-2} was only ~20% of its original thickness. This value is far below the 45%, which could be achieved by a uniaxial stretching at 75°C and atmospheric pressure, as shown in the *Figure*. When the X-ray diffraction patterns were taken at atmospheric pressure for the samples once compressed at 25°C and at different pressures (3000, 5000, and 10 000 kg cm^{-2}) and were compared with those shown in *Figure* 9, the corresponding X-ray diffraction patterns were found to be almost identical to each other. This suggests that the structural changes caused by the compressional plastic deformation were mainly responsible for the observed changes in the X-ray diffraction patterns of the samples under compressional stress states. In order to study the crystal structure of the compressed sample in more detail, therefore, the compression apparatus which was shown in *Figure* 3 and is capable of preparing the samples with larger sizes for X-ray, i.r., and piezoelectric measurements, was used mainly rather than

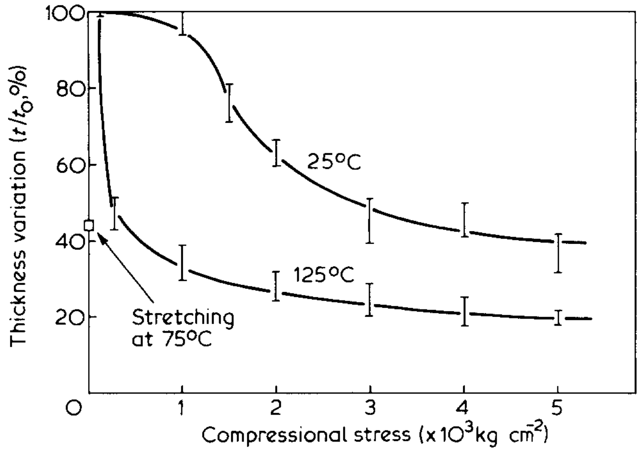

Figure 10 The thickness variations in the samples compressed at various compressional stresses and at the two temperatures 25 and 125°C. Also, the value observed for the sample stretched at 75°C, atmospheric pressure, is shown

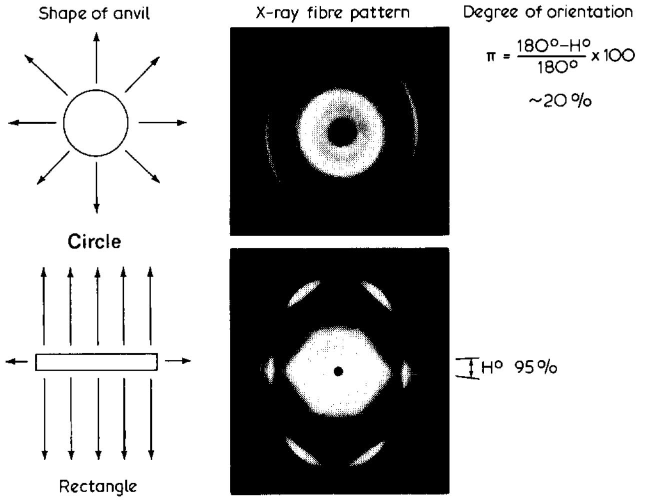

Figure 11 The influence of the shape of compressional anvils on a deformation mode of samples. The samples were compressed at the same condition of 5000 kg cm^{-2}, 125°C

the Be anvil compression apparatus in the following experiments.

Generally, the compressional deformation mode depends not only on compression temperatures and pressures, but also on the shapes of compression anvils, so the effects of anvil shapes on the molecular orientation and the crystal transformation of the compressed samples were studied qualitatively using two different shapes (circle and rectangle), as shown in *Figure* 11. The experiments were performed under the same compressional condition of 5000 kg cm^{-2} and 125°C. When the sample was compressed with circular anvils, the sample deformed in radial directions and the observed X-ray fibre pattern was diffuse. However, when the rectangular shaped anvils were used, the X-ray fibre pattern from the resultant sample was very clear, with a degree of *c*-axis orientation of ~95%, suggesting that the sample deformed almost uniaxially perpendicular to the major direction in the rectangle due to directional friction between the anvils and film surfaces. Although the shapes of the anvils had a strong influence on the X-ray fibre patterns, i.r. spectra observed for these two samples compressed with different anvil shapes, were almost identical to each other.

The X-ray fibre pattern of the sample compressed with rectangular anvils at 5000 kg cm^{-2} and 125°C, which was shown in *Figure* 11, is very similar to that of the sample stretched at atmospheric pressure[4]. Also, the calculated lattice constants coincided with the values reported for Form I crystal[6,7], ascertaining that uniaxial compression has caused a crystal transformation from Form II to Form I in PVDF samples. In spite of a very close resemblance in the X-ray diffraction patterns, i.r. measurements revealed that the crystal structure of the compressed sample might be slightly different from that of the stretched sample. *Figure* 12 compares the i.r. spectra from the samples (a) compresseed at 25°C, 5000 kg cm^{-2}, (b) compressed at 125°C, 5000 kg cm^{-2}, and (c) stretched at 75°C, at atmospheric pressure. The i.r. spectrum from sample (b) corresponds well with the spectrum reported for Form I crystal[8], while that from sample (a) contains i.r. bands from Form II crystal (filled circles in the *Figure*). Similarly, sample (c) contains relatively small quantities of Form II crystal, judged from its i.r. spectrum. Therefore, although these three samples contain different contents of Form II crystal, they were verified at being mostly Form I crystal. Nevertheless, detectable differences exist in intensities of 440 and 470 cm^{-1} bands (filled triangles in the *Figure*) between the i.r. spectra of sample (c) and samples (a) and (b). Although these bands are assigned to be a wagging mode of CF$_2$ and rocking modes of CF$_2$ and CH$_2$ in Form I crystal, respectively[8], it is difficult to correlate the observed differences in the i.r. spectra to fine differences in crystal structures between the sample compressed at high pressure and the one stretched at atmospheric pressure.

In order to study quantitatively the compression temperature effect on the crystal conversion ratio, film samples (50 μm in thickness) were compressed in the temperature range 25–150°C at a constant stress of 5000 kg cm^{-2}. The resultant samples were examined with i.r. spectroscopy and the crystal contents of Form I and Form II were estimated from the observed spectra. In calculating the optical densities of 3022 (an antisymmetric stretching mode of CF$_2$) and 2980 cm^{-1} (a symmetric stretching mode of CH$_2$) bands were utilized as internal standards to normalize the optical densities of key bands in Form I and Form II crystals from the resultant samples with different film thickness. The sample melt-crystallized at atmospheric pressure and the one annealed at 4000 kg cm^{-2} [13] were employed as complete crystals of Form II and Form I, respectively. As shown in *Figure* 13, the relative content of Form I crystal in the compressed

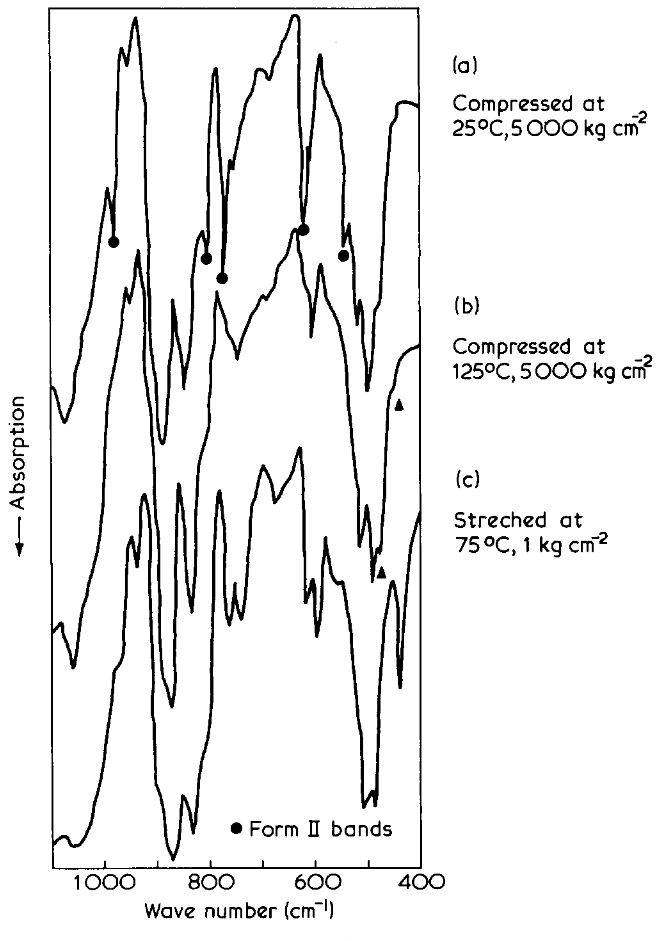

Figure 12 I.r. spectra of samples (a), (b) and (c). ●, indicates the i.r. bands assigned to Form II crystal

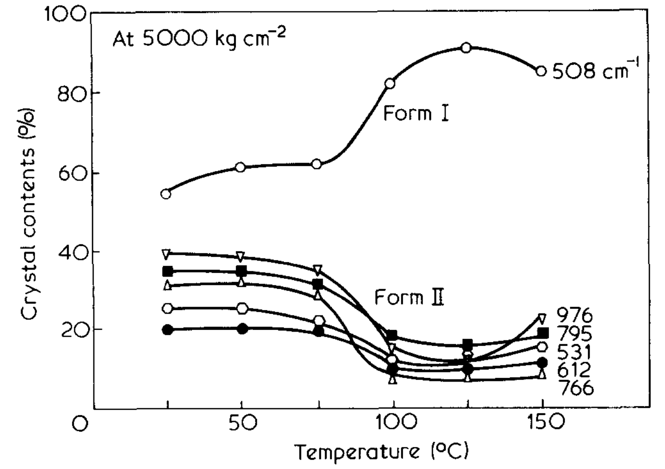

Figure 13 The effect of drawing temperature on relative contents of Form I and Form II crystals in the compressed samples. The values were estimated from the observed i.r. spectra. The samples were compressed at constant stress of 5000 kg cm^{-2} and at different temperatures between 25 and 150°C

samples increased from ~60–90% with increasing compression temperature, while that of Form II crystal decreased from ~30–10%. The maximum crystal conversion was achieved by compression at ~125°C. This fact is in marked contrast to the case of crystal transformation by stretching at atmospheric pressure, where at high stretching temperatures above 140°C the crystal transformation to Form I could not be observed, as described previously. In order to account for this discrepancy between the temperature effects on the crystal transformation by the compression and stretching deformations, differences in the molecular deformation mechanisms and stress distributions in the samples, and other various factors seem to be involved.

As described above, the compression method was shown to produce an oriented Form I crystal from an unoriented Form II crystal by a relatively simple procedure. Furthermore, the anvils of the compression apparatus were always in close contact with the surfaces of the film sample and the anvils could be electrically insulated against each other. Therefore, a poling procedure could be performed on the sample even during the compressional process, so that a piezoelectric film could be prepared in a single operation. Based on these considerations, simultaneous compression and poling operations were actually tried using the anvils with a rectangular shape under the conditions of 125°C, 5000 kg cm^{-2}, and 20 MV m^{-1}. The resultant sample exhibited a piezoelectric stress constant two or three times higher than the value observed for the sample prepared by stretching at 75°C, atmospheric pressure, and then poled at an equivalent condition. A further study on this subject is now in progress and detailed results will be published soon.

SUMMARY

Simultaneous X-ray and stress–strain measurements during a tensile deformation made at atmospheric pressure have elucidated a close correlation between the crystal transformation from Form II to Form I and the deformation mechansim. The crystal transformation was observed only in the temperature range where the sample deformed by cold-drawing and its initiation was detected at the deformation stage where necking was initiated at the centre of the tensile sample, suggesting that a heterogeneous (shear) stress component in the sample played a critically important role in this crystal transformation phenomenon.

It was also confirmed by X-ray and i.r. measurements that uniaxial compressional deformation also causes the crystal transformation from Form II to Form I in PVDF samples. This compression method has the considerable advantage that a high d.c. voltage can be applied to the sample simultaneously with the compressional deformation, resulting in a highly uniaxially oriented Form I crystal film with advanced piezoelectric properties.

ACKNOWLEDGEMENTS

This work was supported in part by a Grant in Aid of Science Research from the Ministry of Education. We are grateful to Professor T. Oyama of Kyushu University for use of his i.r. instrument.

REFERENCES

1 Kondrashov, Yu. D. *Trans. Gipkh'a* 1960, **46**, 166
2 Gal'Perin, Ye. L., Strogalin, Yu. V. and Mlenik, M. P. *Vysokomol. Soedin.* 1965, **7**, 933
3 Makarevich, N. I. and Nikitin, V. N. *Vysokomol. Soedin.* 1965, **7**, 1673
4 Lando, J. B., Olf, H. G. and Peterlin, A. *J. Polym. Sci.* (*A*-1) 1966, **4**, 941
5 Doll, W. W. and Lando, J. B. *J. Macromol. Sci.* (*B*) 1968, **2**, 219; *ibid*, 1970, **4**, 889
6 Hasegawa, R., Kobayashi, M. and Tadokoro, H. *Polymer J.* 1972, **3**, 591
7 Hasegawa, R., Takahashi, Y., Chatani, Y. and Tadokoro, H. *Polymer J.* 1972, **3**, 600
8 Kobayashi, M., Tashiro, K. and Tadokoro, H. *Macromolecules* 1975, **8**, 158
9 Matsushige, K. and Takemura, T. *J. Polym. Sci.* (*Polym. Phys. Edn.*) 1978, **16**, 921
10 Matsushige, K., Nagata, K. and Takemura, T. *Jpn. J. Appl. Phys.* 1978, **17**, 467
11 Kawai, H. *Jpn. J. Appl. Phys.* 1969, **8**, 975
12 Miyata, S., Tasaka, S., Ando, Y., Sakaoku, K. and Fukada, E. 'Extended Abstracts, International Workshop on Electric Charges in Dielectrics', 1978, p 96
13 Matsushige, K. and Takemura, T. *Rep. Prog. Polym. Phys. Jpn.* 1978, **21**, 345